Vol. 12 (núm. 1) pp. 135-142
Enero-Junio 2021

Ciencia en Desarrollo
Revista de la Facultad de Ciencias
Vicerrectoría en Investigación y Extensión - VIE
Centro de Investigaciones y Extensión de la Facultad de Ciencias - CIEC

https://doi.org/10.19053/01217488.v12.n1.2021.12417

Glycerol Oxidation by Fluorinated and Platinized Titania

Oxidación de glicerol mediante titania fluorizada y platinizada

E. Bautista[1], E. G. Ávila-Martínez[2], R. Natividad[1], J. J. Murcia[2], R. Romero[1], J. Cubillos[2], J. S. Hernández[2], O. Cárdenas[3], M. C. Hidalgo[4], J. A. Navío[4], and R. Baeza-Jiménez[2]

Abstract

In this work, fluorinated and platinized TiO_2 were evaluated in the glycerol oxidation. Fluorination led to increasing the specific surface area of titania, and platinization treatment to obtaining the highest absorption in the visible region of the electromagnetic spectrum; thus, 0.5 wt% Pt-F-TiO_2 was the best catalyst for its highest yield and good selectivity to glyceraldehyde (GAL). It was also found that 2 wt% of Pt content had a detrimental effect on the glycerol conversion. Fluorination and platinum addition led to modify the reaction mechanism and selectivity.

***Keywords*:** glycerol, 0.5 wt % Pt-F-TiO_2, 2wt % Pt-F-TiO_2, glyceraldehyde, dihydroxyacetone

Resumen

En este trabajo se evaluó el TiO_2 fluorado y platinizado en la oxidación de glicerol. La fluoración condujo al aumento de la superficie específica de titania y el tratamiento de platinización a obtener la mayor absorción en la región visible del espectro electromagnético; por tanto, 0,5 % en peso de Pt-F-TiO_2 fue el mejor catalizador por su rendimiento más alto y buena selectividad para gliceraldehído (GAL). También se encontró que el 2 % en peso del contenido de Pt tenía un efecto perjudicial sobre la conversión de glicerol. La fluoración y la adición de platino llevaron a modificar el mecanismo de reacción y la selectividad.

***Palabras clave*:** glicerol, 0,5 % en peso de Pt-F-TiO_2, 2 % en peso de Pt-F-TiO_2, gliceraldehído, dihidroxiacetona

Recepción: 15-jul-2020
Aceptación: 31-oct-2020

[1]Centro Conjunto de Investigación en Química Sustentable UAEM-UNAM-México
[2]Grupo de Catálisis, Escuela de Ciencias Químicas, Universidad Pedagógica y Tecnológica de Colombia UPTC. Corresponding author e-mail: julie.murcia@uptc.edu.co
[3]Grupo de Fisicoquímica molecular y modelamiento computacional, Escuela de Ciencias Químicas, Universidad Pedagógica y Tecnológica de Colombia
[4]Instituto de Ciencia de Materiales de Sevilla (ICMS), Consejo Superior de Investigaciones Científicas CSIC, Universidad de Sevilla

1 Introduction

Currently, the excess of glycerol coming from biodiesel industry represents a serious problem, so to develop innovative applications to utilize this compound is a serious challenge for scientific community. Some authors have reported successful studies on this topic. Pagliaro et al., for example, have described the production of 1,3-dihydroxyacetone and hydroxypyruvic acid by glycerol oxidation and the improvement of cements by bioglycerol addition. Kenar [3] also has reported the obtention of different organic compounds from glycerol partial oxidation.

The main catalysts of interest for glycerol oxidation appear to focus on carbon-supported Pt, Pd or Au and bimetallic catalysts such as Au-Pd and Au-Pt [4]. As a result of the use of aqueous glycerol solutions as raw material, glyceric acid, dihydroxyacetone, tartronic acid, and hydroxypyruvic acid have been reported as the main reaction byproducts [5]. These results depend on different properties of the catalysts employed such as particle size and on the reaction conditions; thus, Ketchie et al. have shown the highest selectivity to glyceric acid by using a 1 wt% Au (5-50 nm)/graphite materials [6].

In the present work, TiO_2 has been tested for glycerol oxidation, as the strategies for improve the oxidizing power and physicochemical properties of this oxide, fluorination and incorporation of platinum nanoparticles were employed.

Titania is a well-known material employed in different eco-friendly processes, this is because of its stability, strong oxidizing power and relative low cost [7-16]. In order to improve the properties of TiO_2, metal doping, fluorination and sulfation are suitable alternatives for increasing the specific surface area and the absorption of the oxide in the visible region of the electromagnetic spectrum [7, 12, 13].

2 Methodology

2.1 Catalysts preparation

2.1.1 TiO_2

Hydrolysis of 200 mL of titanium tetraisopropoxide (Aldrich, 97%) in isopropanol solution (1.6 M) was achieved by distilled water addition (isopropanol:water 1:1, V/V). The material obtained was labeled as sg-TiO_2. It was recovered by filtration, drying at 110 °C overnight and calcination at 650 °C for 2 h, 4 °C/min was employed as the heating rate.

Commercial TiO_2 P25 Evonik (TiO_2 (C)) was employed as the reference material with no additional treatment.

2.1.2 F-TiO_2

Fluorinated TiO_2 (F-TiO_2), was obtained from an aqueous suspension of fresh sg-TiO_2 (2g) in 1 L of 10 mM NaF solution; the pH was adjusted to 3 by using a solution 1 M of HCl (in order to improve the fluoride adsorption) [12,13]; this suspension was maintained in the dark under continuous stirring for 1 h. The powders were recovered by filtration, dried and calcined at 650 °C for 2 h, 4 °C/min was used as the heating rate.

2.1.3 Pt addition

Platinum addition was carried out by using Hexachloroplatinic acid (H_2PtCl_6, Aldrich 99.9%) as the metal precursor. For this procedure, a suspension of the F-TiO_2 sample in distilled water containing 0.3 M of isopropanol (Merck 99.8%) was employed. The necessary amount of metal precursor to obtain nominal Pt loading of 0.5 and 2 wt% on TiO_2 was added to this suspension. Metal photodeposition was performed under N_2 flux (0.90L/h), under illumination for 120 min. Light intensity on the suspension was 60 W/m^2 measured by using a photo-radiometer Delta OHM, HD2102.1. An Osram Ultra-Vitalux lamp (300 W) was used as the light source, with a main emission line in the UVA range at 365 nm. The materials obtained were recovered by filtration and dried at 110 °C for 12 h. These materials were labeled as 0.5 Pt-F-TiO_2 and 2 Pt-F-TiO_2.

2.2 Catalysts characterization

The study of catalysts prepared was carried out by using different analytic techniques such as: TEM, S_{BET}, XRD, UV-Vis DR spectrophotometry, XRF and XPS. The analysis parameters have been extensively reported at [12, 13].

2.3 Catalytic reactions

Glycerol oxidation was carried out in an open glass cylindrical reactor (2 cm ID, 20 cm height) fitted with a cooling jacket. A 8 W lamp provided the UV light inside the reactor with a main emission at 254 nm, the energy source was a UVP PS-1 of 115 V/60 Hz and 40 A. All the catalytic tests were carried out in batch mode under continuous stirring. A suspension of the catalysts (TiO_2(C), sg-TiO_2, F-TiO_2, 0.5 Pt-F-TiO_2 and 2 Pt-F-TiO_2) in 100 mL of an aqueous glycerol (J. T. Baker, 99.7%) solution (100 mM) was prepared. The open reactor led the presence of natural room oxygen, room temperature (19 °C) and a starting pH value of 7.8 were employed in all the reactions and the reaction conditions evaluated were: Pt loading (0.5 and 2 wt%) and catalyst amount (10, 30 and 40 mg). Blank tests without catalytic materials were also performed. All the reactions were performed by duplicate.

At the end of each reaction cycle, 90% of the catalysts were recovered by filtration (0.45 μm filter).

2.4 Reaction products determination

1.5 mL were sampled from the reactor at 0, 5, 10, 15, 30, 60, 120, 180, 240 and 300 min, then, these samples were filtered (Sartorius Biolab filters with a pore size of 0.45 μm) and analyzed by High Performance Liquid Chromatography (HPLC) and Total Organic Carbon (TOC). The analytic parameters employed in these techniques are described as follows:

HPLC: 20 μL of each sample were injected in a SHIMADZU Model LC-2030 chromatograph by using an UV 210 nm detector, a SiliaChrom SB C18 column (250 mm length x 5 mm internal diameter x 5 μm Film thickness), 45 °C, an aqueous solution 0.01 mM of H_2SO_4 was employed as mobile phase, flow rate of 0.5 mL/min and total elution time of 10 min.

HPLC standards: Aqueous solutions of Glycerol (G) J. T. Baker, 99.7%, Glyceraldehyde (GAL) Sigma-Aldrich, $>$ 90%, Dihydroxyacetone (DHA) Sigma-Aldrich 97%, Glycolic acid (GA) Sigma-Aldrich, 70 wt% in water, and Formic acid (FA) Honeywell $>$ 98%.

The concentration of reactive and by products was determined by integration of the data by using the Prominence I de SHIMADZU Labsolutions software. Robustness, precision and accuracy studies were performed; from this calculation it was possible to found a variation coefficient lower than 2%, showing the reliability of the measurements. The next equations were employed to determine the glycerol conversion, yield and selectivity:

$$Conversion\ (\%) = \frac{Initial\ concentration\ of\ Glycerol - Final\ concentration\ of\ Glycerol}{Initial\ concentration\ of\ Glycerol} * 100 \quad (1)$$

$$Yield\ (\%) = \frac{Product\ concentration}{Initial\ concentration\ of\ Glycerol} * 100 \quad (2)$$

$$Selectivity\ (\%) = \frac{Yield}{Glycerol\ conversion} * 100 \quad (3)$$

TOC: 100 μL of each sample were injected in an Analytikjena Multi N/C 2100/1 equipment, by using a furnace temperature of 750 °C. Each sample was measured by triplicate and the average value was considered. Catalysts recycling analyzes were not carried out because the low catalyst loading employed (10, 30 or 40 mg); representing the loss of almost 10% of catalyst in each test, makes non-viable this kind of experiments.

3 Results and discussion

3.1 Physicochemical properties from the catalysts characterization

The results from catalysts characterization have been previously reported [12, 13], so, a summary of the more relevant results is presented as follows.

Pt nanoparticle sizes: Selected TEM images of Pt-F-TiO_2 catalysts are presented in Figure 1,

where platinum particles appear as small black spots, which are heterogeneously distributed, with zones presenting many particles and other empty zones on TiO_2 surface. The average particle size has been previously reported of 6 nm [12, 13] and over 7 nm for the 0.5 Pt-F-TiO_2 and 2 Pt-F-TiO_2 catalysts, respectively; Pt nanoparticles in the sample with 2 wt% of platinum content (2 Pt-F-TiO_2) show the highest particles aggregation.

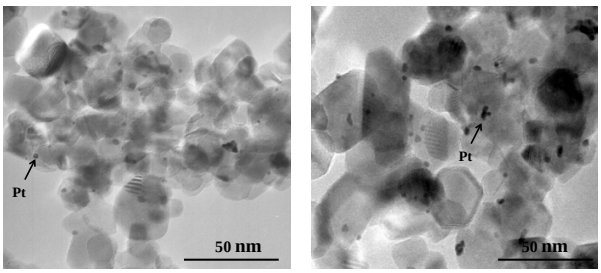

Figure 1. Selected TEM images of Pt-F-TiO_2 catalyst. 0.5 Pt-F-TiO_2 (a) and 2 Pt-F-TiO_2 (b).

Specific surface area: In Table 1 it is possible to observe that the lowest value for specific surface area (S_{BET}) corresponds to 11 m^2/g in the sg-TiO_2 sample, due to titania particles sintering which occurs during the calcination of the bare material. On the contrary, after fluorination, the S_{BET} value considerably increases to 51 m^2/g, thus showing the protective effect of the fluorine ions over the S_{BET} TiO_2 S_{BET} at high temperature [8]. Specific surface area of F-TiO_2 slightly decreases after Pt addition, thus indicating the obstruction of TiO_2 surface by platinum nanoparticles; this effect is less evident in the catalyst with 2 wt% of Pt loading, where the higher Pt size particles produces less obstruction of F-TiO_2 surface.

Table 1. Characterization results summary

Materials	Specific surface area (m^2/g)	$D_{Anatase}$ (nm)	Band gap (eV)	Binding energy (eV)	
				Ti $2p_{3/2}$	O 1s
TiO_2 (C)	51	22	3.23	458.5	529.8
sg-TiO_2	11	17	3.30	458.5	529.8
F-TiO_2	51	24	3.21	458.4	529.6
0.5 Pt-F-TiO_2	42	23	3.24	458.3	529.6
2 Pt-F-TiO_2	50	22	3.26	461.3	531.2

Crystalline phases: Rutile and anatase with a ratio of 90/10 are present in the TiO_2 (C) and sg-TiO_2 samples, these crystalline phases are identified by the main XRD peaks located at 25.25 ° (JCPDS card no. 21-1272) and 27.44 ° (JCPDS card no. 21-1276), respectively (Figure 2).

Rutile phase formation takes place in the sg-TiO_2 sample by titania particles sintering during the calcination at high temperature, which is also associated with the lowest specific surface area observed in this material. In the fluorinated and platinized samples, the fluorine ions protect the titania surface and therefore only anatase phase of TiO_2 was identified, which is in agreement with previous reported results [11, 18].

The lowest anatase crystallite size value corresponds to 17 nm in sg-TiO_2 sample (Table 1), also due to the particle sintering and formation of Rutile phase in this catalyst [12, 13]. On the other hand, fluorinated TiO_2 presents the highest anatase crystallite size due to the presence of fluoride, which can enhance the crystallization of anatase phase and promote the growth of its crystallites [11,18]. Pt addition did not modify significantly the anatase crystallite size.

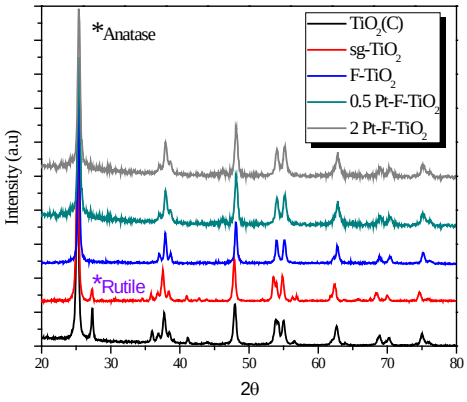

Figure 2. XRD analysis for commercial, lab prepared and modified TiO_2.

Optical properties: The absorption band edge of the TiO_2 is observed in Figure 3 around 400 nm for all the materials analyzed. Due to the presence of fluoride species (Ti ≡ F) on TiO_2 surface, the UV-Vis absorption of the fluorinated samples is slightly higher than that of the sg-TiO_2 material. It was also observed that metallization leads to an increase in absorption in the visible range of the electromagnetic spectrum, due to the grey color of Pt-F-TiO_2 materials.

The band gap energies are reported in Table 1, which are between 3.21 and 3.26 eV, very close to that of anatase TiO_2 (3.20 eV).

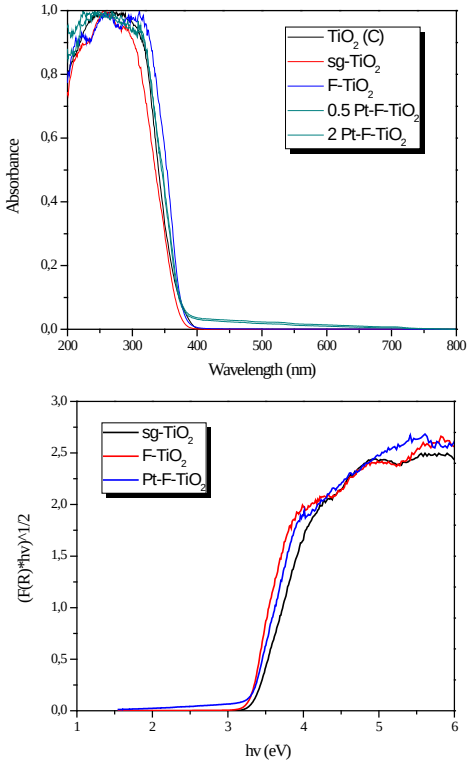

Figure 3. UV-Vis DR spectra of materials prepared.

Chemical content: In the materials analyzed it was possible to detect traces of Cl^- species (0.02%) from the metal precursor (H_2PtCl_6). The Pt content values are lower than the nominal metal loading, thus indicating an incomplete reduction of the metal on the TiO_2 surface during the synthesis process. The real Pt content in the samples was close to 0.39 and 1.25 wt% in the 0.5 Pt-F-TiO_2 and 2 Pt-F-TiO_2, respectively.

XPS: The Ti 2p core peaks presents for all the catalysts the main component at 458.5 $\pm$ 0.1 eV (Ti $2p_{3/2}$), which is typical of the Ti^{4+} ions in the TiO_2 lattice; no modifications were observed after Pt addition. A peak at 529.8 $\pm$ 0.2 eV is assigned to oxygen atoms in the TiO_2 lattice, surface OH groups were also identified in the O 1s region by a shoulder at higher binding energy.

Reduced and oxidized Pt species were detected in the platinized samples, as it is represented in Figure 4.

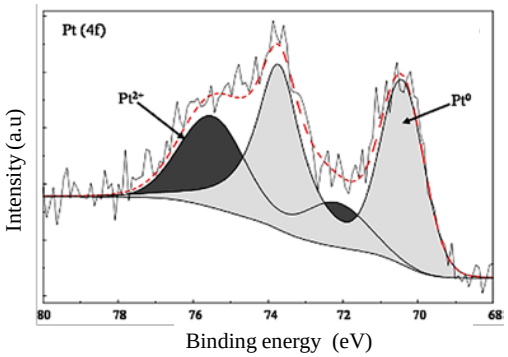

Figure 4. XPS spectra of the region Pt4f in platinized catalysts analyzed.

3.2 Catalytic performance

Firstly, tests without illumination and in presence of a catalyst were carried out and no products were observed, but a slight decrease in the glycerol concentration was observed due to the adsorption of this compound in the catalyst surface.

The highest glycerol transformation was observed in the blank test performed without catalyst, the final glycerol concentration after 300 min of reaction was 11.4 mM, obtaining 8 by-products. G, DHA, GAL and FA concentrations, glycerol conversion, and yield and selectivity of the products are summarized in Table 2.

Figure 5 represents the glycerol concentration as a function of the reaction time over each catalyst. The lowest glycerol transformation (i.e. 79.3 mM) was obtained by using 2 Pt-F-TiO_2 as catalyst.

On the other hand, it was observed that under illumination and in the presence of a catalyst, the glycerol reaction mechanism can be modified. By using sg-TiO_2 or commercial TiO_2 the glycerol is transformed into FA at the first 15 min of reaction, then, DHA and other compounds are produced. When F-TiO_2 is employed as catalyst only DHA and FA were produced; with platinized catalyst also GAL is produced.

As it can be seen in Table 2, the highest glycerol (i.e. 88.4%) takes place in the blank test. The highest yields for GAL and DHA, were achieved with 0.5 Pt-F-TiO_2 catalyst.

Table 2. Conversion, yield and selectivity in Glycerol oxidation reaction. Total reaction time of 300 min

Materials tested	Glycerol conversion (%)	Yield (%)				Selectivity (%)			
		GAL	DHA	FA	Other products	GAL	DHA	FA	Other products
Photolysis	88.40	0.12	6.60	12.80	68.90	0.13	7.51	14.50	77.90
linewidth TiO_2 (C) (10 mg)	82.20	0.00	15.20	12.90	54.00	0	18.50	15.80	65.70
linewidth sg-TiO_2(10 mg)	83.50	0.00	15.16	21.24	54.7	0	16.64	23.31	49.87
linewidth F-TiO_2 (10 mg)	69.40	0.00	9.23	60.20	0	0	13.30	87.00	0
linewidth 0.5 Pt-F-TiO_2(10 mg)	57.40	30.40	24.91	2.10	0	52.98	43.39	3,63	0
linewidth 2 Pt-F-TiO_2(10 mg)	20.40	12.03	0	8.33	0	59.10	0	40.83	0
linewidth 0.5 Pt-F-TiO_2 (30 mg)	34.11	15.45	8,60	10.10	0	45.32	25.16	29.51	0
linewidth 0.5 Pt-F-TiO_2 (40 mg)	14.83	14.83	0	0	0	0	0	0	0

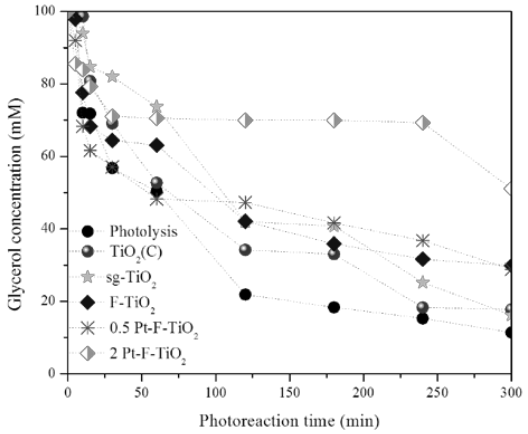

Figure 5. Glycerol concentration evolution over the materials analyzed.

An intermittent behavior was observed over platinized materials, where glycerol concentration increases and then decreases, which can be due to a highest reactive surface, so, glycerol oxidation can be a reversible reaction. This behavior can be explained taking into account that in platinized materials coexist reduced and oxidized Pt species, as it was identified by XPS; these species can define the course of the reaction acting as active sites.

3.3 Effect of the Pt content

Figure 6 shows the evolution of the glycerol oxidation products as a function of reaction time over the catalysts analyzed. It is observed that fluorination and Pt addition on TiO_2 decrease glycerol conversion, but Pt significantly increases the yield to GAL and DHA (Table 2), which very important taking into account the potential applications of these compound at industrial level [2, 19, 20]. It is important to note that in the present work by F and Pt addition to TiO_2 it was possible to increase the selectivity, thus leading to obtain a minor number of byproducts, compared with previous results reported by other authors using different catalytic materials [5].

It is also observed that the Pt loading has an important role in the effectiveness of the F-TiO_2 for glycerol oxidation reaction. By using the 0.5 Pt-F-TiO_2 catalyst, a glycerol conversion of 57.40%, and a yield of 30.40, 24.91 and 2.1 to GAL, DHA and FA, respectively, were obtained. On the other hand, by using 2 Pt-F-TiO_2, both the conversion and yield to the products significantly decreases. This can be due to the glycerol adsorption on catalyst surface, thus, it is possible that $Pt^{\delta+}$ species can favor the adsorption of glycerol molecule.

As it was observed by TEM, Pt particle size is related with metal loading, and the catalyst presenting the bigger Pt nanoparticles (2 Pt-F-TiO_2) led to the lowest glycerol transformation. Liang et al. [21] have found that bigger sized Pt particles (> 10 nm) were less active, whereas smaller sized ones (< 6 nm) exhibited higher glycerol conversion and stable selectivity.

3.4 Effect of the catalyst loading

The results obtained by using different catalyst amount (i.e. 10, 30 and 40 mg) in the glycerol oxidation reaction over 0.5 Pt-F-TiO_2 catalyst are presented in Table 2. It was observed that glycerol

conversion and yield to the GAL, DHA and FA decreases as the catalyst loading increases, this behavior is due to a screening effect, which masks part of the photosensitive area inside the reactor, thus reducing the effectiveness of the process in the glycerol oxidation reaction.

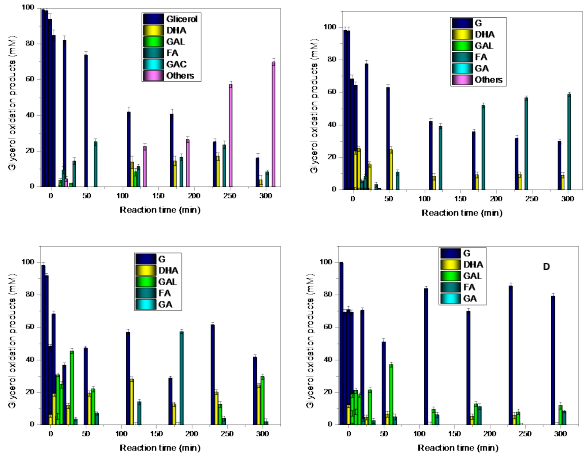

Figure 6. Glycerol and oxidation products concentration as a function of the catalytic oxidation time. (A) sg-TiO_2; (B) F-TiO_2; (C) 0.5 Pt-F-TiO_2 and (D) 2 Pt-F-TiO_2.

3.5 Mineralization

All the glycerol oxidation reactions were monitored by the Total Organic Carbon (TOC) analyzes, from this technique it was observed that CO_2 or H_2 did not produced in any of the reactions performed, so, the mineralization was never reached.

4 Conclusions

Glycerol can be transformed under illumination producing eight different compounds, but, when a catalyst based on TiO_2 is added to reaction medium, the number of products significantly decreases.

Fluorination and platinization are treatments that can modify the physical properties of TiO_2 prepared by sol-gel method, thus, a high absorption in the visible region of the electromagnetic spectrum and high surface area are obtained.

It was also observed that fluorine ions and Pt nanoparticles have an important role in the reaction mechanism and selectivity during glycerol oxidation.

The general behavior in glycerol oxidation can be summarized as follows: (i) the use of commercial or lab prepared TiO_2 as catalysts led to three intermediaries products after 60 minutes of reaction; (ii) fluorine addition on TiO_2 surface, led to the formation of DHA and FA; (iii) when Pt was added to F-TiO_2 GAL, DHA and FA were produced.

By increasing the Pt loading from 0.5 to 2 wt% glycerol conversion and the intermediaries products yield decrease; it can be related to the better adsorption of glycerol on 0.5 wt% Pt-F-TiO_2 catalyst.

10 mg was the best loading for glycerol oxidation over 0.5 wt% Pt-F-TiO_2, this amount is enough to avoid the screening effect inside the reactor.

Acknowledgments

Authors thanks to Universidad Autónoma del Estado de México (UAEM), grant number 3892/2015 FS, this work was also financed by Fondo Nacional de Financiamiento para la Ciencia, la Tecnología y la Innovación Francisco José de Caldas-Colciencias, Project 279-2016, and Universidad Pedagógica y Tecnológica de Colombia project SGI 2006.

References

[1] M. Rossi, C. Della-Pina, M. Pagliaro, R. Ciriminna, P. Forni, “Greening the Construction Industry: Enhancing the Performance of Cements by Adding Bioglycerol”, *Chem. Sus. Chem., 1,* p. 809-812, 2008.

[2] R. Ciriminna, G. Palmisano, C. Della-Pina, M. Rossi, M. Pagliaro, “One-pot electrocatalytic oxidation of glycerol to DHA”, *Tetrahedron Lett.*, *47*, p. 6993-6995, 2006.

[3] J.A. Kenar, “Glycerol as a platform chemical: Sweet opportunities on the horizon?”, *Lipid Technol., 19*, p. 249-253, 2007.

[4] M. Bowker, C. Morton, J. Kennedy, H. Bahruji, J. Greves, W. Jones, P. R. Davies, C. P. Brookes, P. Wells, N. Dimitratos, “Hydrogen production by photoreforming of biofuels using Au, Pd and Au-Pd/TiO_2 photocatalysts”, *J. Catal., 310*, p. 10–15, 2014.

[5] S. Demirel-Gülen, M. Lucas, P. Claus, "Liquid phase oxidation of glycerol over carbon supported gold catalysts" *Catal. Today.*, *102*, p. 166-172, 2005.

[6] W. C. Ketchie, M. Murayama, R. J. Davis, "Selective oxidation of glycerol over carbon-supported AuPd catalysts", *J. Catal.*, *250*, p. 264-273, 2007.

[7] M. Maicu, M. C. Hidalgo, G. Colón, J. A. Navío, "Comparative study of the photodeposition of Pt, Au and Pd on pre-sulphated TiO_2 for the photocatalytic decomposition of phenol", *J. Photochem. Photobiol., A.*, *217*, p. 275-283, 2011.

[8] D. Li, H. Haneda, S. Hishita, N. Ohashi, N.K. Labhsetwar, "Fluorine-doped TiO_2 powders prepared by spray pyrolysis and their improved photocatalytic activity for decomposition of gas phase acetaldehyde", *J. Fluorine Chem., 126*, p. 69-77, 2005.

[9] K. Okazaki, Y. Morikawa, S. Tanaka, K. Tanaka, M. Kohyama, "Effects of stoichiometry on electronic states of Au and Pt supported on TiO_2(110)", *J. Mater. Sci. 40, p.* 3075-3080, 2005.

[10] J. J. Murcia, J. R. Guarín, A. C. Cely Macías, H. Rojas, J. A. Cubillos, M. C. Hidalgo, J. A. Navío, "Methylene blue degradation over M-TiO_2 photocatalysts (M = Au or Pt)", *Ciencia en Desarrollo*, *8*, p. 109-117, 2017.

[11] J. Yu, Q. Xiang, J. Ran, S. Mann, "One-step hydrothermal fabrication and photocatalytic activity of surface-fluorinated TiO_2 hollow microspheres and tabular anatase single microcrystals with high-energy facets", *Cryst. Eng. Commun.*, *12*, p. 872-879, 2010.

[12] J. J. Murcia, M. C. Hidalgo, J. A. Navío, J. Araña, J. M. Doña-Rodríguez, "Study of the phenol photocatalytic degradation over TiO_2 modified by sulfation, fluorination, and platinum nanoparticles photodeposition", *Ap. Catal., B.*, *179*, p. 305–312, 2015.

[13] G. Iervolino, V. Vaiano, J. J. Murcia, L. Rizzo, G. Ventre, G. Pepe, P. Campiglia, M. C. Hidalgo, J. A. Navío, D. Sannino, "Photocatalytic hydrogen production from degradation of glucose over fluorinated and platinized TiO_2 catalysts", *J. Catal.*, *339*, p. 47-56, 2016.

[14] M. N. Chong, V. Vimonses, S. Lei, B. Jin, C. Chow, C. Saint, "Synthesis and characterisation of novel titania impregnated kaolinite nano-photocatalyst", *Micropor Mesopor Mat., 117*, p. 233-242, 2009.

[15] J. Fernández, J. Kiwi, J. Baeza, J. Freer, C. Lizama, H. D. Mansilla, "Orange II photocatalysis on immobilised TiO_2: Effect of the pH and H_2O_2", *Ap. Catal. B, 48*, p. 205-211, 2004.

[16] R. Molinari, F. Pirillo, M. Falco, V. Loddo, L. Palmisano, "Photocatalytic degradation of dyes by using a membrane reactor", *Chem. Eng. Process, 43,* p. 1103-1114, 2004.

[17] S. P. Tandom, J. P. Gupta, "Measurement of forbidden energy gap of semiconductors by diffuse reflectance technique", *Physica Status Solidi B. 38,* p. 363-367, 1970.

[18] M. S. Vohra, S. Kim, W. Choi, "Effects of surface fluorination of TiO_2 on the photocatalytic degradation of tetramethylammonium", *J. Photochem. Photobiol., A., 160*, p. 55-60, 2003.

[19] A. Behr, J. Eilting, K. Irawadi, J. Leschinski, F. Lindner, "Improved utilisation of renewable resources: new important derivatives of glycerol", *Green Chem.*, *10,* p. 13–30, 2008.

[20] V. Augugliaro, H. A. Hamed, V. Loddo, A. Mele, G. Palmisano, L. Palmisano, S. Yurdakal, "Partial photocatalytic oxidation of glycerol in TiO_2 water suspensions", *Catal Tod. 151,* p. 21-28, 2010.

[21] D. Liang, J. Gao, J. Wang, P. Chen, Z. Hou, X. Zheng, "Selective oxidation of glycerol in a base-free aqueous solution over different sized Pt catalysts", *Catal. Commun.*, *10, p.* 1586-1590, 2009.